The Phusor®-type LANR Cathode is a Metamaterial Creating Deuteron Flux for Excess Power Gain

Mitchell Swartz and Gayle Verner
JET Energy, Inc. Wellesley, MA 02481(USA)

Abstract - The spiral Phusor®-type LANR cathode, with open helical geometry in a high electrical impedance solution, creates a unique electric field distribution. This results in both deuteron loading flux from the solution and an intra-palladium deuteron flux at equilibrium. The stereoconstellation of the LANR electrode augments material factors, and makes a LANR 'metamaterial'. The intra-electrode palladium flux drives some of the desired LANR reactions.

Index Terms - lattice assisted nuclear reactions; LANR; LENR; palladium; deuterium; Phusor®-type LANR cathode; deuteron loading; metamaterial

1.1 Metamaterials and LANR Defy Expectations

Metamaterials [1-24] and hydrogen-loaded Group VIII alloys that exhibit "lattice assisted nuclear reactions" (LANR) [25-42] have surprising, physical characteristics that defy earlier expectations, yet each produce solid, indelible experimental results. Their precisely engineered materials and structures have characteristic behavior far beyond what is normally expected, making previously-"impossible" effects such as negative refractive index [1,2] and electromagnetic cloaking [3] occur. Similarly, reports of excess energy and nuclear reactions from solid state LANR [25-42] were initially felt to be impossible, but growing experimental evidence suggests otherwise. Active LANR devices produce helium-4 [25,26,35,46], tritium [31,27,28,33] as nuclear ash, very small amounts of emissions [29,30], and hundreds of thousands of joules of 'excess heat' per day [37,41,39]. This paper reports that both effects are secondary to the stereoconstellation used. In LANR, we report a unique E-field distribution can be generated to provide intra-palladium deuteron flux, linked to successful LANR results.

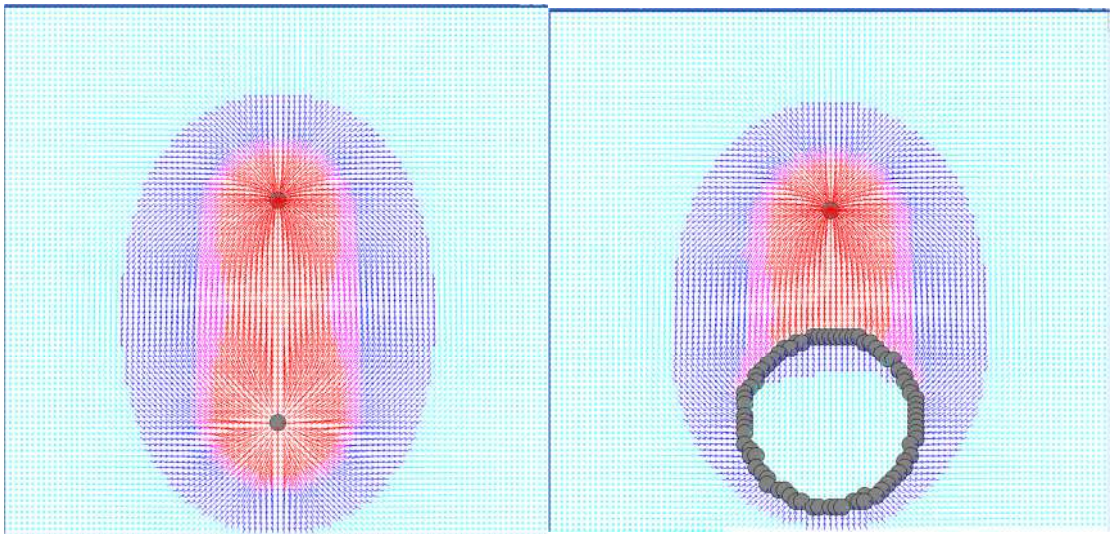

Figure 1. Electric field distributions for wire-wire and wire-Phusor®-type system

1.2 Metamaterials

Metamaterials defy previous expectations, creating negative refractive index materials [1,2], electromagnetic cloaking (and not just screening) [3], a simultaneous negative phase and group velocity of light [4], anomalous reflections and excitations of surface waves [5], isotropic lenses [6], and soliton decoherence [7]. Electrical permittivity, ε, and magnetic permeability, μ, are both positive in nature [8]. In such normal materials, classic physics principles use the right-handed rule for electromagnetic (light) propagation, with the energy [Poynting vector; 9] traveling in the same direction. However, if a material is a "left-handed material" (LHM), then it has a negative (refractive) index material (NIM), and other unusual things occur. In left-handed materials (LHM), both ε and μ are negative, and the phase and group velocities of light propagate in opposite directions [10]. This has been observed for metamaterials with their left-handed properties [11] where the handedness makes light propagate opposite the Poynting vector (energy flows), and enables reversal of the expected Doppler shift, and causes Cherenkov radiation, normally emitted in the forward direction, to be emitted backwards [12].

Metamaterials come in both arrays [13-16] and sol-gel composites [17]. They are useful in electrical engineering, making novel antennas, filters, waveguides, and artificial magnetic media, composed of a split-ring resonator (SRR) lattice with negative permeability over a certain frequency range [14]. Metamaterials have been engineered in the optical to mid-IR range with fabrication by nanoimprint lithography [18,19], using perforated SiC membranes [20], into broadband devices of right/left-handed metamaterials [21]. Devices have even been designed using planned zero refraction metamaterials [22], and second-harmonic generation from magnetic metamaterials [23,24].

The important point is not that ε, μ, or the group velocity, or the group velocity of light are negative in this system or electrode, or that the Phusor®-type metamaterial LANR structure necessarily involves composites or sol-gels, but that metamaterials, through their unique, novel structures, can make previously "impossible" effects occur. Conventional metallurgy and

material science accrue from the “internal structure of cathode material”, whereas metamaterials result from the precisely crafted and planned external structure.

1.3 Does Phusor Metamaterial Structure Create Material properties?

We have tried many designs and variations of electrodes, arrangements and materials, but the uniquely-shaped spiral Phusor®-type cathodic structure has stood out for reproducibility, activity, and power gain. Its arrangement and stereo-constellation of electrodes appears to be one of the better arrangements for a LANR system, measured by activity and power gain [37,38,41,39]. We previously reported that unique well localized, small-area bubble coverage has been correlated with successful LANR-active Pd/D_2O/Pt, Pd/D_2O/Au, and Ni/D_2O,H_2O/Pt Phusor®-type devices operation. This has been confirmed by heat flow measurement, calorimetry, electrical and mechanical energy conversion devices, and dual serial calorimetry.

The Phusor®-type LANR device, with its helical, cathodic design and low electrical conductivity solution, is the most successful half-electrochemical system we have found judged by robust excess heat production and reproducibility. Why? We investigated that issue.

Our hypotheses for its superior function included the cold working, the preparation, Frenkel defects, and the possibility of specific alterations in the electric field intensity distribution. Metamaterials may have begun in the optical and microwave areas but we elected to take a closer theoretical, calculated look at their use here for energy production and conversion. The hypothesis examined here is that the metamaterial helix electrode might be interacting with the applied electrical field intensity distribution. We report below a theoretical investigation which indicates that our best LANR devices, these cathodes used with a very high resistance solution, are indeed a metamaterial.

2. Experimental – First Order E-field Analysis

A set of experiments were set up to theoretically determine why the Phusor®-type LANR setup gave superior results. Examined was the effect of geometric parameters, of both the wire-wire and wire-Phusor system (Figure 1), upon the electrical field distribution. Metamaterials have been studied using ab initio numerical simulation [60]. In other non-metamaterial systems, electric field intensity computations using Laplace's equation for a variety of geometries [61-63] are well known. Important considerations include that of a “Conducting Circular Rod in Uniform Transverse Field”, and “Approximate Current Distribution around Relatively Insulating and Conducting Rods” [61]. More complicated systems have been analyzed in several ways. Such electric field computations have been undertaken by numerical analysis of the polarizability characteristics for dielectric circular cylinders through an integral equation for the scalar potential [64]. This is done by calculating the polarization charge surface density in a Fourier series, with the related coefficients, the so-called multipoles, obtained from a linear set of equations [65], by analytic calculations, for two parallel dissimilar cylinders in an electrolyte solution on the basis of a linearized Poisson-Boltzmann equation [66], by adding to the linear Poisson-Boltzmann equation further consideration of the electrostatic potential and the energy of such a charge distribution[67], by a two-term Galerkin solution, for a hollow conducting tube of finite length held at a fixed potential [68], by a conformal mapping that converts the

actual boundary-free field zone into a rectangular domain [69], by imaging [70], and by dyes sensitive to the electric potential [71].

There are limitations in this analysis. First, only *ab initio*, first order, electric field distributions were qualitatively examined for obvious differences that might be present secondary to structure. The goal was not to perform a quantitative Gouy determination, nor to examine near surfaces, nor in double layers. Second, no closed-form solution probably exists because this is a dynamic system with secondary dielectric effects because conduction and polarization are linked (through Hilbert Space [72]), and because of convection, and time variant thermal and Bernard instability issues.

Our gendanken computed simulation used Laplace electrostatic calculations away from the electrodes, away from the interface, and outside the double layers. These were not quantitative calculations of the electric field's magnitude, which are difficult in a time-variant system with solution conduction/polarization changes. Nor were they an attempt to determine fine structure within the interfacial regions, but a first order extension of the, previous described and successful Q1D model of isotope loading [55,56], to now include intrapalladial deuteron flow, similar to holes and electrons in semiconductors, within the loaded electrode. Although classical electrostatics analysis indicates that a perfect conductor does not have an electric field within it, the real palladium cathode is not a perfect conductor. We measure the palladium electrical conductivity by four terminal measurements which, for these Phusor cathodes, range from 40 to ~120 milliohms.

This theoretical examination considered the Pd spiral, immersed and bathed, like the platinum anode, in the high electrical resistivity solution, relatively electrically insulating, for the most general case of two infinitely long electrodes, placed in a vertical, parallel position. We modeled the device as an electrically conductive ring of cylindrical symmetry (open at some angle for each 2D cut) of infinite length. Using boundary conditions and superposition, the electric field distribution was calculated to first order, qualitatively, in two dimensions. When the field distribution was analyzed 'around the electrode' this means also an examination as a function of angular distribution around the electrode with the electrode's center as the angular center.

3.1 Results - Distinguishing E-fields Suggest Possible Metamaterial

The Phusor®-type LANR device is a metamaterial and its physical structure enhances the metallurgic properties of loaded palladium. This metamaterial change alters the electric field distribution, producing continuous deuteron flux within the loaded palladium. This is unique to this device creating a distinguishing electric field (E-field) distribution different from customary wire-wire, and other systems. The electric field distributions are shown in Figure 1 which shows in cross-section, the derived first order 2-Dimensional (2D) vector electric field distributions for the two cases. The first case is that of two parallel, infinitely long, wire electrodes (anode at the top, and cathode below). The second case is a wire-Phusor system. In cross-section, the complex structure is approximated. The anode is at the top, and the cathode in each pair is located below it. Each cathode is electrically polarized against, and physically

located opposite, an anodic wire of platinum. The colors show several arbitrary thresholds in electric field intensity.

The results of this analysis show the 2D E-field distribution and deuteron flux sequelae vary greatly between the wire-wire system and the wire-metamaterial ystem. The 2-D E-field distributions reveal there are important differences between the electrostatic distributions produced by the two arrangements of wire-wire versus wire-Phusor. In a 2D view around the cathode wire, there is a near isotropic distribution of the E-field. With the Phusor, there is not. In the configuration examined in this present investigation has revealed that in the helical system there is a direct, loading, electric field intensity results in those portions of the cylinder which are closest to the wire; this extends over a solid angle over a two dimensional angle of approximately ~45°-130°, depending on many factors of the Phusor geometry and precise inter-electrode distance.

The result is a clear deuteron flux through that portion of the cathode, which does not characterize the two wire situation over as large a volume. With the metamaterial configuration, there is a flux of deuterons resulting in a quite different performance than conventionally described, or expected, in electrochemistry using simpler structures such as wires.

Referring to Figure 2, consistent with electrostatics, the fluxes of deuterons in the solution (J_D) and in the metal, both for loading (J_E), gas evolution (J_G), and fusion (J_F, are now augmented by an equilibrium intrapalladial deuteron flux (J_{IP} in Figure 2); therein a possible rub for hydrogen isotope energy production reactions.

3.2 Results - E-Field Distribution Change

Our experimental results and theoretical analysis have suggested that the spiral helical structure and geometric arrangement of the palladium Phusor®-type electrode, located opposite a platinum anode may be part of the arrangement which yields unusually high excess heat in this type of LANR system (37). The theoretical analysis has determined that there is a uniqueness to the design of the cathode, with its open helical geometry and orientation in a high electrical resistivity solution. These alter the 2-D electric-field intensity (E-field) spatial distribution uniquely and perhaps enable the desired reactions to occur. The pericathodic E-field distribution becomes less isotropic in 2 dimensions. The portion of the cathode vicinal to the anode, off axis, may sustain a higher than normal internal electric field intensity within its bulk lattice volume.

In this case, metamaterial issues including geometry and stereoconstellation augment metallurgy of the loaded Pd cathodes. Something unexpected happens: successful LANR experiments, and a possible explanation for the more reproducible, and higher excess energy production.

3.3 Results - Deuteron Flow Distribution Change

The metamaterial aspect of these LANR devices appear to enable them to be more fully loaded, and the structural geometry interacting with the applied electric field intensity produces

a net continuous flux of deuterons moving through the palladium. With the metamaterial LANR cathode there is an equilibrium intrapalladial deuteron flow, in addition to --and after-- deuteron loading through portions of the cathode. Two deuteron flows are created by the Phusor®-type LANR cathode. The first is the standard deuteron interelectrode (between electrodes) loading flux, beginning in the solution and ending in the metal lattice. This is driven by the applied electric field intensity. The second is an additional intraelectrode deuteron flux, through the metal, itself. This intrapalladial deuteron flow continues at equilibrium, similar to the microscopic equilibrium semiconductor flux of holes and electrons at a p-n junction. We now suspect that this additional type of deuteron flow is critical and enabling to LANR results. The results here support this. So do the results of Violante [46] and Iwamura [34].

3.4 Results - Deuteron Flux

Deuteron flux has been examined in metal scandium films, where buildup of deuterium in the near-surface area is controlled by migration to deeper depths [73], in niobium membranes [74], and in molybdenum, below 500 K, deuterium retention is enhanced by trapping at defects produced by the deuterium bombardment; above 500 K, the implanted deuterium is immediately released [75]. There has been a need to study these deuterium fluxes in palladium systems. Nernst calculations of the activities of electrolyte [76,77] adjacent to a metal electrode have been applied to LANR [36] to derive distributions of deuterium in the palladium [30] and solution [55,79]. However, the LANR systems are not at equilibrium, and Nernst calculation may not be applicable [55,56]. Also, a vicinal reference electrode may herald the Nernst potential, but probably not the loading flux rate (which will be shown below to be key to these reactions). Therefore, a quasi-one-dimensional (Q1D) model for hydrogen loading of an electrode was formulated [55], which does not require equilibrium for accuracy. The Q1D model describes the loading flux of hydrogen by the ratio of two energies (electric order to thermal disorder ratio).

Figure 2 is a schematic, simplified, representation of the anode, solution, and a portion of the cathode along with five types of deuteron fluxes involved in loading, D_2 evolution, and putative fusion; in solution and the palladium. The figure shows the deuteron cationic flow (J_D), and the four types of deuteron flux in the loaded palladium cathodic lattice (J_E, J_G, J_F, and J_{IP}). Deuteron flux (J_D) begins far from the cathode surface, in the deuterium oxide (heavy water) located between the electrodes, where the deuterons are tightly bound to oxygen atoms as D_2O. There is no additional solute. In the absence of significant solution convection, the flux of deuterons (J_D) results from diffusion down concentration gradients and electrophoretic drift by the applied electric field [55,80]. Cationic deuteron flux (J_D) brings deuterons to the cathode surface, from the heavy water as D-defects [81,82] are driven by the applied electric field intensity to create a cathodic fall and double layer before the electrode surface.

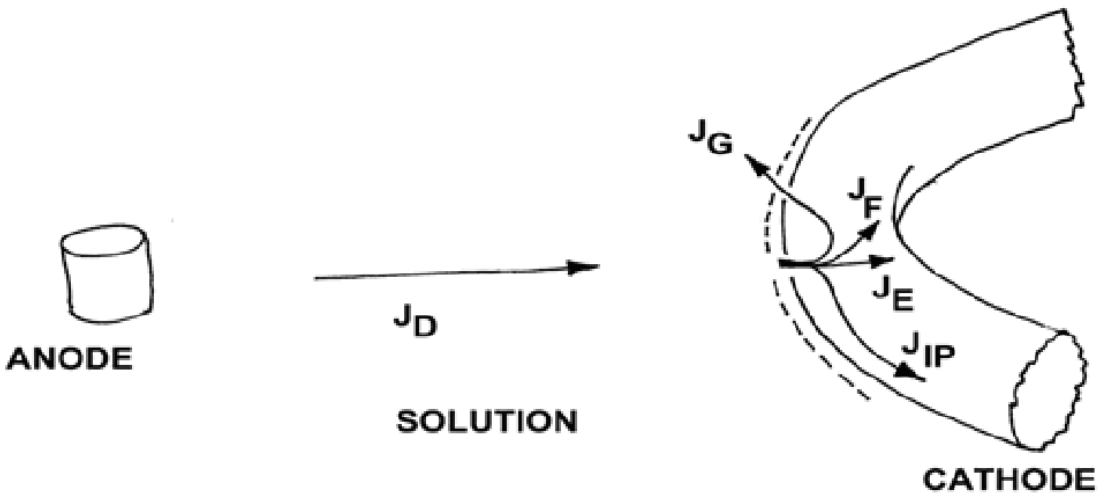

Figure 2. Schematic Model of the Five Types of Deuteron Flux

From the metallurgical point of view (POV), from the metal surface, atomic deuterons either enter the metal ("are loaded"), remain on the surface, or form diatomic deuterium gas bubbles (D_2). The gas bubbles (D_2) are undesirable producing low dielectric constant layers in front of the electrode, obstructing the electrical circuit. And so, at the metal surface, four components of deuteron flux must be considered [55,56], fundamental to the entire understanding of these phenomena. These deuteron fluxes include entry into the metal (J_E), movement to gas evolution (J_G), and an extremely tiny loss by potential fusion reactions (J_F). There is conservation of deuterons with the exception of a loss (J_F) to all putative fusion reactions, which are extremely small, if present. With this paper, we now add the concept of a continuous, equilibrium, flux of deuterons within the cathode (J_{IP}), which may be consistent with excess heat and an observed unusual bubbling pattern (see below).

The important point is that different deuteron fluxes must be distinguished [55] at the surface of the low hydrogen-overvoltage palladium, with its surface populated with atomic, diatomic (D_2), and bulk-entering deuterons [83,84]. This paper expands the Q1D model of loading to include the possibility of intrapalladial deuteron flow at equilibrium.

3.5 Results - Deuteron Flux Equation Predicts LANR is NOT Electrolysis.

From the mathematical POV, the three components of flux are the entry of deuterons to the lattice (J_E), gas evolution (J_G), and the desired fusion reactions (J_F). Dividing each flux by the local deuteron concentration yields the first order deuteron flux constants, k_E, k_G, and k_F [cm/sec], respectively, which are the basis of the rest of the discussion, and Equation 2.

$$J_D = -B_D * \frac{d[D(z,t)]}{dz} - \mu_D * [D(z,t)] * \frac{d\Phi}{dz} \quad \text{Equation 1}$$

The deuteron flux, J_D, depends on deuteron diffusivity (B_D) and electrophoretic mobility (μ_D), and the applied electric field intensity. At any molecular site across the heavy water solution, the applied electrical energy is a tiny fraction compared to k_B*T, so the deuterons migrate by drift ellipsoids of L- and D-deuteron defects in the applied electric field creating a ferroelectric inscription [81,82]. This D-defect conduction/polarization process augments other charge carriers, ionic drift, space charge polarization, and clathrates. The resultant D-defect migration produces a "cathodic fall" of deuterons and a E-field contraction so that most of the voltage drop is at the interface in front of the electrode surface. This concentration polarization may produce very large local electric field intensities, possibly ranging from 10^4 to 10^7 volt/cm [55].

From the concentration polarization of deuterons before the cathode, the Pd loads, controlled by the double layer, which limits the entry of deuterons to the metal surface. At the inner boundary of the double layer, intermolecular deuteron transfer from the heavy water solution to the metal surface, coupled by electron-limited transfer, leaves an atomic deuteron on the metal surface. This leaves an atomic deuteron attached to the metal surface, and the electrode metallurgy controlled by the tiny interfacial region, which might be less than 10 Angstroms thick, by the applied electric field intensity, and by the local concentration of deuterons. The entry mechanisms to the palladium surface are driven by infrared vibrations and microwave rotations [55], creating a solution photosensitivity which produces a photoactivated increase of excess energy and loss of power gain [42].

Palladium has its surface populated with atomic (D) and diatomic deuterium (D_2). A large number of those deuterons can also enter the metal forming a binary alloy [83, 84]. Deuterons which enter (load) into the palladium lattice are 'dressed' by a partial electronic cloud, shielding their charge (Born-Oppenheimer approximation). The deuterons drift along dislocations and through the lattice and its vacancies, falling from shallow to deeper located binding sites. There is obstruction by ordinary hydrogen and other materials at interfaces and grain boundary dislocations.

$$\kappa_e = (\mu_D * E) - (\kappa_g + \kappa_f) \qquad \text{Equation 2}$$

Equation 2 is the deuteron loading rate equation. It relates cathodic deuteron gain from the applied electric field to the loss of deuterons from gas evolution and fusion, and teaches many things. The deuteron loading rate equation shows that the deuteron gain of the lattice [through the first order loading flux rate (k_E)] is dependent upon the applied electric field MINUS the flux rate losses of deuterons from gas evolution (k_G) and fusion (k_F). The deuteron loading rate equation, Equation 2, reveals that desired LANR reactions are quenched by electrolysis, which is opposite conventional “wisdom” that LANR is 'fusion by electrolysis'.

Equation 2 also heralds that LANR can be missed by insufficient loading, contamination (effecting k_E, by protons or salt), and by the evolution of D_2 gas, which all inhibit the desired LANR reactions [55], and leading to the optimal operating point manifolds.

$$k_e = \frac{B_D * qV}{L * [k_B * T]} - (\kappa_g + \kappa_f)$$

Equation 3

The modified deuteron flux equation [Equation 3] is Equation 2 changed by substituting the Einstein relation, which makes for an equation reminiscent of semiconductor physics at p-n junctions. The first term now has geometric, material factors, and the ratio of two energies [the applied electric energy organizing the deuterons divided by k_B*T, thermal disorder].

The modified deuteron flux equation reveals how competitive gas evolving reactions and the applied electric field energy to thermal energy [k_B*T] are both decisive in controlling the deuteron loading flux in palladium. Successful LANR experiments are dominated by this ratio reflecting the 'war' between applied electrical energy which is organizing the deuterons versus their randomization by thermal disorganization. The two terms are the first order deuteron loss rates by gas evolution and the desired fusion process(es).

There are several important implications and opportunities. This paper discusses the idea of an equilibrium flux of deuterons within the cathode (J_{IP}), and we believe that this internal, intraelectrode rather than interelectrode, flux may be the cause of what has been observed with excess heat and bubbling (discussed below).

First, this paper expands the Q1D model, and our understanding of these deuteron flows and their role in hydrogen energy by now including the possibility of secondary microscopic equilibrium deuteron flux within the metal, an intrapalladial deuteron flow. This is similar to holes and electrons in semiconductors, and their equations involving the Einstein relation (cf. Equation 3) are also similar. The Phusor®-type cathode is a unique LANR metamaterial, whose stereoconstellation connects deuteron loading to other fluxes of deuterons continuing to move inside of the palladium, just as holes and electrons move in a semiconductor.

Second, Equation 3 is similar to some flux equations from semiconductor physics, so there is the question of similarity of deuterons in Pd to holes and electrons in semiconductors.

Third, this metamaterial view of these cathodes may explain their relatively-reproducible excess energy production compared to other LANR systems, thereby opening up new routes to improved hydrogen energy production by LANR. Finally, although not all of the controlling factors of LANR success have been elucidated, this paper adds a new control point, deuteron flux within the lattice from an applied electric field intensity within an electrochemical LANR cell.

3.6 Results - Role of Bubble Coverage

Bubble formation has a large controlling role in electrochemistry [85], in part because the adhering bubbles, isolate the electrode [86]. In fact, at high current densities, bubble evolution

is a rate limiting step, dependant upon whether the bubbles coalesce or not [87]. Under microgravity conditions or if acidic solutions are used, large bubbles are formed, coalesce and remain on the cathode surface [88,89]. Alkaline solutions make bubble froth [89]. Bubble coverage has a great role in LANR [37]. The bubbles interfere with competitive reactions, including loading. Reduction reactions are also competed with by such bubbling, e.g. in ferricyanide solutions on platinum [90,91]. The activation energy appears to be in the range of 56 kJ/mol-1 (electrodeposited Ni on Pt) to 204 kJ/mol-1 (electrodeposited Hg on Pt) [92].

3.7 Results - Limited-area, Large-Bubble Coverage

Figure 3 shows a close-up of an active Phusor®-type spiral-wound excess-heat-producing palladium cathode. The Pt anode is to the left of the cathode, and is not shown in the photograph, as discussed in detail [37]. A high electrical resistivity solution, located between the two electrodes, bathes the metamaterial cathode, including within the spiral.

There is seen very limited, well localized, small area large-bubble (asymmetric) coverage bubbling vs. normal bubbling [37]. There are bubbles only on one side of the cathode, what we call “asymmetric bubbling” which differs from normal bubbling. With LANR success, at current densities of 1.5×10^{-4} to ~0.13 amperes/cm^2, we have observed behavior similar to what is seen in microgravity or acidic solutions. This is seen at relatively high voltages. Plasmas have not been observed, unless the cathode, or anode, are suddenly removed from the solution during the run at high voltage.

We postulated in 2003 that this unique type of cathodic bubble behavior, “Asymmetric Electrolysis”, heralds, and drives, intrapalladial deuteron flux deuteron flux through that portion of the loaded metal cathode. Thus, it is could be used as a sign of LANR success for some excess-heat-producing cathodes as experimentally observed and reported, and openly demonstrated at ICCF-10 [37,41].

The present paper goes further and provides confirmatory, theoretical and experimental, support (Figures 1,3). First, this paper reports that Phusor®-type-LANR generated metamaterial-derived intrapalladial flux in the cathode does appears to be heralded by small bubble evolving area on the surface of palladium and linked to activity of LANR cathodes [Figure 3]. This putative hypothesized intrapalladial deuteron flux is corroborated with this paper whose results show the asymmetric electric field distribution at the front of the (facing the anode).

Intrapalladial deuteron flux may have implications for palladium loading [37,55,56], for monitoring that loading, and regarding the likelihood of success. By contrast, many electrochemists have generally been more concerned with 'throwing power' of their systems and solutions, rather than focusing on improving active LANR behavior. Generally, in solutions of more electrical conductivity, with materials other than palladium, and with no possibility to load (or create other desired reactions), one sees, at hundreds of volts applied yielding a current density of ~10^{-5} amperes/cm^2, tiny bubbles over the cathode, beginning at select, preferred sites.

In the future, metamaterial intrapalladial flux may offer new types of devices (like p-n junctions). In LANR, metamaterial function should now be considered as a method to improve efficiency, yielding a new spectrum of devices using equilibrium intraelectrode deuteron flow. This may also open up new routes to improved control of LANR systems.

4. Interpretation and Conclusion

E-Field Distribution Change

The Phusor®-type LANR metamaterial design with its spiral cathode system-wire anode system, with its open helical cylindrical geometry, creates a unique and unusual electric field distribution superior in performance. There is an anomalous effect in those portions of the cathode closest to the anode. In some configurations, this extends over an angle of circa 45°-130° degrees. This results in both interelectrode deuteron flux from the solution to the electrode for loading and intra-palladium deuteron flux (after full loading).

Deuteron Flow Distribution Change

Confirming the intraelectrode deuteron flux, analysis reveals that the Phusor®-type shape effects outcome, as confirmed by the calculated E-field distributions. There is the possibility that changes resulting from the geometry and stereoconstellation of the cathode material may be a factor, and may account for the relative success of this system. In addition, the understanding, and engineering, of these two types of deuteron flows is critical to new key components for successful LANR, and perhaps other hydrogen, energy production results.

Metamaterial Role in LANR and Hydrogen Energy Production

Geometry, stereoconstellation, and location of electrodes, metamaterial issues, are now shown to play additional possible roles in successful LANR experiments. The findings of this paper's theoretical research, supplementing much experimental work involving the Phusor-heavy water system including with respect to spatial distribution of D_2 evolution and excess heat production, suggests these designs are metamaterials. Here the electrode metamaterial function appears to help produce more successful and efficient, LANR systems by generating additional types of equilibrium deuteron flux, a possible additional *sine qua non* for the desired reactions in successful LANR reactions. We believe that intra-electrode palladium flux is what is necessary to produce the desired reactions, and that such a flux is often missed in competing systems, based on our experimental results here, and a review of the poorer performance of some competing systems.

Thus, there are several connections between metamaterials in general, Phusor®-type LANR structures in particular, and then hydrogen energy devices in general, LANR devices in particular. First, the results, theoretically and experimentally, suggest that in the pursuit of hydrogen energy, the metamaterial function may be important and augment the material properties by improving efficiency.

The second important point is that in addition to past patterns of failure of LANR systems, from excessive electrical conductivity of the solution, to failure to drive the system near its OOP, to failure to adequately load, now metamaterial issues should also be considered.

Third, consideration of metamaterial structure and stereoconstellation of the electrode system might engineer alteration of the two types of deuteron flows for the ultimate design of future, more successful, LANR materials and devices. In fact, researchers of LANR, hydrogen energy production systems, and the solid state have a new way to think about their systems, and a possible new spectrum of devices using intraelectrode deuteron flow.

Acknowledgments

The authors thank Allen Swartz, Alex Frank, Isidor Straus, Steven Olasky, Peter Hagelstein, Marcus Zahn, Brian Ahern, David Nagel, Larry Forsley, Pamela Mosier-Boss, and Brian Josephson who have given critique, support, ideas and suggestions, and JET Energy and the New Energy Foundation for their additional support. PHUSOR® is a registered trademark of JET Energy, Incorporated. PHUSOR®-technology is protected by U.S. Patents D596724, D413659 and U.S. Patents pending.

REFERENCES

1. D.R. Smith, J.B. Pendry, M.C.K. Wiltshire, “Metamaterials and Negative Refractive Index”, Science (2004) sciencemag.org.
2. “Experimental Verification of Backward-Wave Radiation From a Negative Refractive Index Metamaterial”, Journal of Applied Physics (2002) waves.utoronto.ca.
3. D. Schurig, J.J. Mock, B.J.Justice, S.A. Cummer, J.B., “Metamaterial Electromagnetic Cloak at Microwave Frequencies”, Science (2006) sciencemag.org.
4. G. Dolling, C. Enkrich, M. Wegener, C.M. Soukoulis, “Simultaneous Negative Phase and Group Velocity of Light in a Metamaterial”, Science,(2006). sciencemag.org.
5. G. Brodin, M. Marklund, L. Stenflo, P.K. Shukla, “Anomalous Reflection and Excitation of Surface Waves in Metamaterials” Physics Letters A, (2007).
6. E. Verney, B. Sauviac, C.R. Simovski, “Isotropic Metamaterial Electromagnetic Lens”, Physics Letters A, (2004).
7. M. Marklund, P.K. Shukla, L. Stenflo, G. Brodin, “Solitons and Decoherence in Left-Handed Metamaterials, Physics Letters A, (2005).
8. A. Von Hippel, “Dielectric Materials and Applications”, MIT Press, Cambridge (1954).
9. J. R.Whinnery, S. Ramo,”Fields and Waves in Modern Radio”, John Wiley & Sons, Inc. New York, Chapman & Hall, Ltd., London, (1953).
10. http://www.fen.bilkent.edu.tr/~ozbay/Papers/60-02apl-LHMbayndir.pdf http://www.fen.bilkent.edu.tr/~ozbay/Papers/70-03-ieee-ozbay_tap_2003.pdf [15] http://www.fen.bilkent.edu.tr/~ozbay/Papers/60-02apl-LHMbayndir.pdf http://www.fen.bilkent.edu.tr/~ozbay/Papers/70-03-ieee-ozbay_tap_2003.pdf http://www.photonics.com/spectra/tech/XQ/ASP/techid.848/QX/read.htm http://ceta-p5.mit.edu/metamaterials/papers/external/2004/Krowne_prl_2004.pdf http://ceta-p5.mit.edu/metamaterials/papers/external/2000/smith.K_prl_2000.pdf http://www.fen.bilkent.edu.tr/~ozbay/Papers/70-03-ieee-ozbay_tap_2003.pdfhttp://www.photonics.com/spectra/tech/XQ/ASP/techid.848/QX/read.htm

http://ceta-p5.mit.edu/metamaterials/papers/external/2004/Krowne_prl_2004.pdf http://ceta-p5.mit.edu/metamaterials/papers/exte nal/2000/smith.K_prl_2000.pdf http://www.fen.bilkent.edu.tr/~ozbay/Papers/70-03-ieee-ozbay_tap_2003.pdf

11. H. Chen, "T-Junction Waveguide Experiment to Characterize Left-Handed Properties of Metamaterials", Journal of Applied Physics, (2003). ceta-p6.mit.edu.
12. J. Pendry, et alia, Defense Advanced Research Projects Agency, http://physics.ucsd.edu/~drs, Air Force Office of Scientific Research (AFOSR).
13. R.A. Shelby, D. R. Smith, S.Schultz, "Experimental Verification of a Negative Index of Refraction", http://physics.ucsd.edu/~drs., Appearing in the April 6, 2001 issue of Science.
14. C.Scott, S. Cummer, http://www.ee.duke.edu/Academics/Undergraduate/IndStudy03/ScottC2003.html "Towards Negative Index Material: Magnetic Response".
15. Negative Index of Refraction In Left Hand Material Composite MetaMaterials Have Unnatural Electromagnetic Properties".
16. http://www-physics.ucsd.edu/lhmedia/how.html
17. J.E. Kielbasa, J. Liu, K.B. Ucer, D.L. Carroll, R.T., "Sol-gel Nanocomposites as Metamaterials: Preparation and Optical Measurements", Journal of Materials Science: Materials in Electronics (2007).
18. W. Wu, E. Kim, E. Ponizovskaya, Y. Liu, Z. Yu, N. Fang, "Optical Metamaterials at Near and Mid-IR Range Fabricated by Nanoimprint Lithography", Applied Physics A: Materials Science & Processing (2007).
19. W. Wu, Z. Yu, S.Y. Wang, R.S. Williams, Y.Liu, C. Sun, "Mid-Infrared Metamaterials Fabricated by Nanoimprint Lithography", Applied Physics Letters,(2007). link.aip.org... mat/pdf/0508/0508307.pdf; R.Marques, F.Medina, and R.Rafii-El-Idrissi
20. D. Korobkin, Y.A, Urzhumov, B. Neuner III, C. Zorman, "Mid-Infrared Metamaterial Based on Perforated SiC Membrane: Engineering Optical Response Using" Z. … - Applied Physics A: Materials Science & Processing (2007).
21. C. Caloz, H.V. Nguyen "Novel Broadband Conventional-and Dual-Composite Right/Left-Handed (C/D-CRLH) Metamaterials", Applied Physics A: Materials Science & Processing (2007).
22. Q. Wu, P. Pan, F.Y. Meng, L.W. Li, J. Wu, "A Novel Flat Lens Horn Antenna Designed Based on Zero Refraction Principle of Metamaterials", Applied Physics A: Materials Science & Processing (2007).
23. M. W. Klein, C. Enkrich, M. Wegener, S. Linden, "Second-Harmonic Generation from Magnetic Metamaterials" all 4 versions, Science (2006). sciencemag.org
24. S. Linden, C. Enkrich, M. Wegener, J. Zhou, T. Koschny, "Magnetic Response of Metamaterials at 100 Terahertz", Science (2004). sciencemag.org
25. M.H., Miles, R.A. Hollins, B.F.Bush, J.J. Lagowski, R.E. Miles, "Correlation of excess power and helium production during D2O and H2O electrolysis using palladium cathodes", J. Electroanal. Chem., 346 (1993) 99-117; Miles, M.H., B.F.Bush, "Heat and Helium Measurements in Deuterated Palladium", Transactions of Fusion Technology, vol 26, Dec. 1994, pp 156-159.
26. M. H. Miles, M.A.Imam, M.Fleischmann, "Calorimetric Analysis of a Heavy Water Electrolysis Experiment Using a Pd-B Alloy Cathode", Proc. Electrochem. Soc. (2001) 2001-23, 194.

27. M. Srinivasan, et alia., “Tritium and Excess Heat Generation During Electrolysis of Aqueous Solutions of Alkali Salts with Nickel Cathode,” Frontiers of Cold Fusion, Ed. by H. Ikegami, Proceedings of the Third International Conference on Cold Fusion, October 21-25, 1992, Universal Academy Press, Tokyo, pp 123-138.
28. S. Szpak, P.A. Mosier-Boss, C. Young, and F.E. Gordon, 'Evidence of Nuclear Reactions in the Pd Lattice', Naturwissenschaften, Vol. 92, pp. 394-397 (2005)
29. S. Szpak, P.A. Mosier-Boss, and F.E. Gordon, 'Further Evidence of Nuclear Reactions in the Pd/D Lattice: Emission of Charged Particles', Naturwissenschaften, Vol. 94, pp. 511-514 (2007).
30. P. A. Mosier-Boss, S. Szpak, F.E. Gordon, L.P.G. Forsley, “Use of CR-39 in Pd/D Co-Deposition Experiments”, Eur. Phys. J. Appl. Phys. 40, (2007) 293-303.
31. S. Szpak, P.A. Mosier-Boss, R.D. Boss, and J.J. Smith, 'On the Behavior of the Pd/D System: Evidence for Tritium Production', Fusion Technology, Vol. 33, pp. 38-51 (1998).
32. Szpak, S., et al., “The effect of an external electric field on surface morphology of co-deposited Pd/D films”, J. Electroanal. Chem., 580: 284-290, (2005).
33. F. G. Will, K. Cedzynska, D.C. Linton, “Tritium Generation in Palladium Cathodes with High Deuterium Loading”, Transactions of Fusion Technology, vol 26, Dec. 1994, pp 209-213; “Reproducible tritium generation in electrochemical cells employing palladium cathodes with high deuterium loading, J. Electroanal. Chem 360 (1993) 161-176.
34. Iwamura, Y., M. Sakano, and T. Itoh, Elemental Analysis of Pd Complexes: Effects of D2 Gas Permeation. Jpn. J. Appl. Phys. A, 2002. 41: p. 4642; Iwamura, Y., et al., “Observation Of Surface Distribution Of Products By X-Ray Fluorescence Spectrometry During D2 Gas Permeation Through Pd Complexes”, in The 12th International Conference on Condensed Matter Nuclear Science. 2005. Yokohama, Japan.
35. Y. Arata and Y.C. Zhang, 'Anomalous Production of Gaseous 4He at the Inside of DS-Cathode During D2-Electrolysis', Proc. Jpn. Acad. Ser. B, Vol. 75, p. 281 (1999); Arata, Y. and Y.C. Zhang, Observation of Anomalous Heat Release and Helium-4 Production from Highly Deuterated Fine Particles. Jpn. J. Appl. Phys. Part 2, 1999. 38: p. L774; Arata, Y. and Y. Zhang, The Establishment of Solid Nuclear Fusion Reactor. J. High Temp. Soc., 2008. 34(2): p. 85.
36. M. Fleischmann, S. Pons, “Calorimetry of the Pd-D2O system: from simplicity via complications to simplicity”, Physics Letters A, 176, 118-129, (1993);M. Fleischmann, S. Pons, “Electrochemically Induced Nuclear Fusion of Deuterium”, J. Electroanal. Chem., 261, 301-308, erratum, 263, 187 (1989); M. Fleischmann, S. Pons, “Some comments on the paper Analysis of Experiments on Calorimetry of LiOD/D2O Electrochemical Cells, R.H.Wilson et al., J. Electroanal. Chem., 332 (1992) 1* “, J. Electroanal. Chem., 332, 33-53, (1992).
37. M. Swartz, G. Verner, “Excess Heat from Low Electrical Conductivity Heavy Water Spiral-Wound Pd/D2O/Pt and Pd/D2O-PdCl2/Pt Devices”, Condensed Matter Nuclear Science, Proceedings of ICCF-10, eds. Peter L. Hagelstein, Scott, R. Chubb, World Scientific Publishing, NJ, ISBN 981-256-564-6, 29-44 (2006).
38. Swartz, M.R. “Excess Power Gain and Tardive Thermal Power Generation using High Impedance and Codepositional Phusor Type LANR Devices”, Proceedings of the 14th International Conference on Condensed Matter Nuclear Science (2010)
39. Swartz, M, “Improved Electrolytic Reactor PerformanceUsing p-Notch System Operation and Gold Anodes, Transactions of the American Nuclear Association, Nashville, Tenn Meeting, (ISSN:0003-018X publisher LaGrange, Ill) 78, 84-85 (1998)

40. M. Swartz, “Consistency of the Biphasic Nature of Excess Enthalpy in Solid State Anomalous Phenomena with the Quasi-1-Dimensional Model of Isotope Loading into a Material”, Fusion Technology, 31, 63-74 (1997).
41. Swartz, G. Verner, “Can a Pd/D2O/Pt Device be Made Portable to Demonstrate the Optimal Operating Point”, ICCF-10 (Camb. MA), Proceedings of ICCF-10, (2003), Condensed Matter Nuclear Science, Proceedings of ICCF-10, eds. Peter L. Hagelstein, Scott, R. Chubb, World Scientific Publishing, NJ, ISBN 981-256-564-6, 45-54 (2006).
42. M. Swartz, G. Verner, “Photoinduced Excess Heat from Laser-Irradiated Electrically-Polarized Palladium Cathodes in D2O”, Condensed Matter Nuclear Science, Proceedings of ICCF-10, eds. Peter L. Hagelstein, Scott, R. Chubb, World Scientific Publishing, NJ, ISBN 981-256-564-6, 213-226 (2006).
43. M. McKubre, F. Tanzella, P. Hagelstein, K. Mullican, and M. Trevithick, 'The Need for Triggering in Cold Fusion Reactions,' Proceedings of the 10th International Conference on Cold Fusion (2003).
44. M. Swartz, “Codeposition Of Palladium And Deuterium”, Fusion Technology, 32, 126-130 (1997).
45. M. Swartz, “Patterns of Failure in Cold Fusion Experiments”, Proceedings of the 33RD Intersociety Engineering Conference on Energy Conversion, IECEC-98-I229, Colorado Springs, CO, August 2-6, (1998).
46. V. Violante, E. Castagna, C. Sibilia, S. Paoloni, and F. Sarto, 'Analysis of Mi-Hydride Thin Film After Surface Plasmons Generation by Laser Technique' ' Proceedings of the 10th International Conference on Cold Fusion (2003).
47. Miley, G.H. and P. Shrestha. Review Of Transmutation Reactions In Solids. in Tenth International Conference on Cold Fusion. 2003. Cambridge, MA, ibid.
48. Swartz, M.R., Gayle Verner, Alan Weinberg, “Possible Non-Thermal Near-IR Emission Linked with Excess Power Gain in High Impedance and Codeposition Phusor-LANR Devices”, Proceedings of the 14th International Conference on Condensed Matter Nuclear Science (2010)
49. Rabinowitz, M., et al. Opposition and Support for Cold Fusion. in Fourth International Conference on Cold Fusion, Lahaina, Maui: Electric Power Research Institute 3412 Hillview Ave., Palo Alto, CA 94304, (1993).
50. M. Swartz, “Phusons in Nuclear Reactions in Solids”, Fusion Technology, 31, (1997) 228-236.
51. Swartz, M, G. Verner, “Bremsstrahlung in Hot and Cold Fusion”, J New Energy, 3, 4, 90-101 (1999)
52. M. Swartz, Science and Engineering of Hydrided Metals Series, Volume 2 - “Calorimetric ComplicationsThe Examination of the Phase-II Experiment and Other Select Calorimetric Issues”, Ed. JET Technology Press, Wellesley Hills, MA, ISBN 1-890550-02-7 (1999); Swartz, M, “Some Lessons from Optical Examination of the PFC Phase-II Calormetric Curves”, Vol. 2, “Proceedings: Fourth International Conference on Cold Fusion”, 19-1, op. cit. (1993)
53. Swartz, M, “A Method To Improve Algorithms Used To Detect Steady State Excess Enthalpy”, Transactions of Fusion Technology, 26, 156-159 (1994)
54. M. Swartz, “Patterns of Failure in Cold Fusion Experiments”, Proceedings of the 33RD Intersociety Engineering Conference on Energy Conversion, IECEC-98-I229, Colorado Springs, CO, August 2-6, (1998).

55. M. Swartz, “Quasi-One-Dimensional Model of Electrochemical Loading of Isotopic Fuel into a Metal”, Fusion Technology (1992) 22, 2, 296-300.
56. M.Swartz, “Isotopic Fuel Loading Coupled to Reactions at an Electrode”, Fusion Technology (1994) 26, 4T, 74-77.
57. M. Swartz, “Control of Low Energy Nuclear Systems through Loading and Optimal Operating Points”, ANS/ 2000 International Winter Meeting, Nov. 12-17, 2000, Washington, D.C. (2000).
58. M. Swartz, “Generality of Optimal Operating Point Behavior in Low Energy Nuclear Systems”, Journal of New Energy, 4, 2, 218-228 (1999).
59. M. Swartz, “Optimal Operating Point Characteristics of Nickel Light Water Experiments”, Proceedings of ICCF-7 (1998).
60. T. Weiland “Ab Initio Numerical Simulation of Left-Handed Metamaterials: Comparison of Calculations and,” Journal of Applied Physics (2001). meta-materials.mit.edu
61. A. Hermann Haus, J. R. Melcher, “Electromagnetic Fields and Energy,” Prentice Hall, Englewood Cliffs, New Jersey.
62. R. B. Adler, L. J. Chu, R. M. Fano, “Electromagnetic Energy Transmission, and Radiation”, John Wiley & Sons, Inc., New York, London, Sydney.
63. S.Ramo, J. R. Whinnery “Fields and Waves in Modern Radio” , John Wiley & Sons, Inc. New York, Chapman & Hall, Ltd.,. London, (1953).
64. J. Venermo and A. Sihvola, “Dielectric Polarizability of Circular Cylinder”, Journal of Electrostatics, 63, Issue 2 (2005) 101-117.
65. S. Giordano, “Multipole Expansions; Composite Materials; Dielectric Homogenisation”, Journal of Electrostatics, 63, Issue 1 (2005), 1-19.
66. H. Ohshima, “Electrostatic Interaction Between Two Parallel Cylinders”, Colloid & Polymer Science, 274, Number 12 (1996).
67. A. G. Cherstvy and R. G. Winkler, “Complexation of Semiflexible Chains with Oppositely Charged Cylinder”, The Journal of Chemical Physics (2004), 120, Issue 19, 9394-9400. Institut für Festkorperforschung, Theorie-Il, Forschungszentrum Jülich, D-52425 Jülich, Germany - In this case for biopolymers, they found that sufficiently flexible chains prefer to wrap around a cylinder in a helical manner, when their charge density is smaller than that of the cylinder. The optimal value of the helical pitch is found by minimization of the sum of electrostatic and bending energies.
68. R.W. Scharstein, “Capacitance of a Tube”, Journal of Electrostatics, 65, Issue 1 (2007) 21-29.
69. L. M. Dumitran, P. Attenb, P. V. Notinghera and L. Dascalescuc, “2-D Corona Field Computation in Configurations with Ionising and Non-Ionising Electrodes”, Journal of Electrostatics, 64, Issues 3-4 (2006) 176-1 86.
70. J.R. Smith, “Electric Field Imaging”, Thesis, Doctor of Philosophy, Massachusetts Institute of Technology (1999).
71. C.B.Chien, J.Pine, Biophys. J., S (1991) 3, 697-711.
72. A. Von Hippel, “Dielectric Materials and Applications”, MIT Press, Cambridge (1954).
73. Cowgill, D.F., Dynamic Ion Beam Method for Measuring Deuterium Diffusion in Films, (1980) IEEE Transactions on Nuclear Science, NS-28 (2), pp. 1851-1185.
74. Bandourko, V., Deuterium permeation through Nb during low energy ion irradiation at controlled surface conditions, (1996) Journal of Nuclear Materials, 233-237 (PART II), pp. 1184-1188.

75. Tanabe, T., Hachino, H., Takeo, M., Behavior of deuterium implanted in Mo, (1990) Journal of Nuclear Materials, 176-77, pp. 666-671.
76. J. O'M Bockris, A. K. N. Reddy, “Modern Electrochemistry”, Plenum Press (1970).
77. H. H. Uhlig, “Corrosion and Corrosion Control”, Wiley (1971).
78. S. Szpak, C.J. Gabriel, J.J. Smith, R.J. Nowak, “Electrochemical Charging of Pd Rods”, J. Electroanal. Chem., 309 (1991) 273-292.
79. M. Viitanen, “A Mathematical Model of Metal Hydride Electrodes”, J. Electrochem. soc., 140, 4, (1993), 936-942.
80. J. R. Melcher, “Continuum Electromechanics”, MIT Press, Cambridge, (1981).
81. A. Von Hippel, D.B. Knoll, W.B. Westphal, “Transfer of Protons through 'Pure' Ice 1h Single Crystals”, J. Chem. Phys., 54, 134, (also 145), (1971).
82. Swartz. M., “Dances with Protons - Ferroelectric Inscriptions in Water/Ice Relevant to Cold Fusion and Some Energy Systems”, Infinite Energy, 44, (2002).
83. Hampel, C.A., “Rare Metal Handbook”, Reinhold Publishing, NY (1954).
84. Hansen, M., K. Anderko, “Constitution of Binary Alloys”, McGraw-Hill, NY (1958)
85. Vogt, H., Balzer, R.J., The bubble coverage of gas-evolving electrodes in stagnant electrolytes, (2005) Electrochimica Acta, 50 (10), pp. 2073-2079. Cited 13 times.
86. Wuthrich, R., Comninellis, Ch., Bleuler, H., Bubble evolution on vertical electrodes under extreme current densities, (2005) Electrochimica Acta, 50 (25-26 SPEC. ISS.), pp. 5242-5246.
87. Wuthrich, Fascio, V., Bleuler, H., A stochastic model for electrode effects, (2004) Electrochimica Acta, 49 (22-23 SPEC. ISS.), pp. 4005-4010.
88. Iwasaki, A., Kaneko, H., Abe, Y., Kamimoto, M., Investigation of electrochemical hydrogen evolution under microgravity condition, (1998) Electrochimica Acta, 43 (5-6), pp. 509-514.
89. Matsushima, H., Nishida, T., Konishi, Y., Fukunaka, Y., Ito, Y., Kuribayashi, K., Water electrolysis under microgravity: Part 1. Experimental technique, (2003) Electrochimica Acta, 48 (28), pp. 4119-4125.
90. Mat, M.D., Aldas, K., Ilegbusi, O.J., A two-phase flow model for hydrogen evolution in an electrochemical cell, (2004) International Journal of Hydrogen Energy, 29 (10), pp. 1015-1023. Cited 9 times.
91. Gabrielli, C., Huet, F., Nogueira, R.P., Electrochemical impedance of H2-evolving Pt electrode under bubble-induced and forced convections in alkaline solutions, (2002) Electrochimica Acta, 47 (13-14), pp. 2043-2048.
92. Correia, A.N., Machado, S.A.S., Hydrogen evolution on electrodeposited Ni and Hg ultramicroelectrodes, (1998) Electrochimica Acta, 43 (3-4), pp. 367-373.